

Oxygen channels of ADEOS-II AMSR: Comparison of the measured and simulated brightness temperatures

M.L. Mitnik and L.M. Mitnik

V.I. Il'ichev Pacific Oceanological Institute FEB RAS, 690041 Vladivostok, Russia – (maia, -mitnik)@poi.dvo.ru

Abstract - Advanced Microwave Scanning Radiometer (AMSR) on a board of ADEOS-II satellite had 14 channels, two of which received outgoing Earth's radiation at an absorption band of molecular oxygen at frequencies $\nu = 50.3$ and 52.8 GHz with vertical (V) polarization. Numerical experiments with a microwave radiative transfer model were carried out at the variations of the atmospheric and ocean surface parameters to interpret the variations of the measured brightness temperatures $T_B(\nu)$ and determine a contribution of the ocean and the atmosphere to the $T_B(\nu)$. Computations have shown that the T_B^V variations reach 32-35 K at $\nu = 50.3$ GHz and decrease till 25-28 K at 52.8 GHz. The potential of oxygen channels is demonstrated by AMSR-based analysis of the cold air outbreaks, convective eddies, extratropical and tropical cyclones.

Keywords: ADEOS-II AMSR, oxygen absorption, brightness temperatures, marine weather systems, tropical cyclones, retrieval algorithms.

1. INTRODUCTION

The Earth's observation in the 50-70 GHz oxygen band was begun after the launch of Nimbus-6 satellite. Scanning Microwave Spectrometer (SCAMS) was installed on its board. It was designed to map tropospheric temperature profiles, water vapor abundance, and cloud water content to be used for weather prediction even in the presence of clouds. The SCAMS continuously monitored emitted microwave radiation at frequencies $\nu = 22.235, 31.65, 52.85, 53.85$ and 55.45 GHz. The three channels near the 5.0-mm oxygen absorption band were used primarily to deduce atmospheric temperature profiles. The ground resolution was ≈ 145 km near nadir and ≈ 330 km at the scan limit.

Although the SCAMS instrument was designed for observation of mid-latitude weather systems, it was used for observation of typhoons too. This instrument could not resolve the eye, but the warm region surrounding the eye was partially resolved. The warm anomaly, which was a result of upper-level warming over tropical storms was detected. In the nadir viewing position the 55.45 GHz channel is most sensitive to atmospheric temperature around 13 km, the 53.85 GHz channel is most sensitive to atmospheric temperature around 5 km, and 52.85 GHz channel is most sensitive to temperature near 2-5 km above the sea surface (Kidder et al., 1978; Rosenkranz et al., 1978).

Further it was shown that the magnitude of the warm anomaly in the microwave data is related to the storm's central pressure and outer winds (Kidder et al., 1978; Velden and Smith, 1983; Velden, 1989; Velden et al., 1991).

Significant progress came to investigation of weather systems when the Advanced Microwave Sounding Unit (AMSU) was launched aboard NOAA-15 on May 1998 and then aboard NOAA-16 and NOAA-17. This satellite instrument has 20 channels, and 8 of them were near the 5.0-mm oxygen absorption band. The spatial resolution was 48 km (Kidder et al., 2000; Knaff et al., 2000; Staelin and Chen, 2000). Such resolution of AMSU provided a detailed map of temperature in tropical cyclone (TC), to estimate a temperature anomaly at its eye, wind speed and so on.

At December 2002 the Advanced Microwave Scanning Radiometer (AMSR) with 14 microwave channels was launched on a board of the Japanese satellite ADEOS II. The $T_B(\nu)$ measurements were carried out at $\nu = 6.9, 10.65, 18.7, 23.8, 36.5, 89.0$ GHz with V- and H-polarization and at $\nu = 50.3$ and 52.8 GHz with V-polarization only. Instant field of view (IFOV) of both oxygen channels was 12×6 km and sampling rate was 10×10 km at all channels with $\nu \leq 50.3$ GHz. An incidence angle of conical scanning $\theta = 55^\circ$ and a swath width was approximately 1600 km.

The purpose of a given work is an estimation of the potential of high-resolution 50.3- and 52.8- GHz channels in combination with other AMSR channels to study the ocean weather systems, in particular, tropical cyclones.

2. MODELING OF MICROWAVE RADIATIVE TRANSFER WITHIN THE RANGE OF 50-55 GHz

The brightness temperature of the ocean-atmosphere system was found from the following formula:

$$T_B^{\nu,H}(\nu,\theta) = \kappa^{\nu,H}(\nu,\theta)T_o e^{-\tau_{\text{sec}\theta}} + T_{\text{Batm}}^{\uparrow}(\nu,\theta) + T_{\text{Batm}}^{\downarrow}(\nu,\theta)[1 - \kappa^{\nu,H}(\nu,\theta)] e^{-\tau_{\text{sec}\theta}} \quad (1)$$

where $\kappa^{\nu,H}(\nu,\theta)$ = sea surface emissivity
 T_o = sea surface temperature
 τ = total atmospheric absorption
 $T_{\text{Batm}}^{\uparrow}, T_{\text{Batm}}^{\downarrow}$ = upwelling and downwelling brightness temperatures of the atmosphere, correspondingly.

The formulas and constants used for computation of atmospheric absorption and the sea surface emissivity are given in (Mitnik and Mitnik, 2003). A microwave radiative transfer model and hydrometeorological database were used to estimate the variations of the brightness temperatures and absorption by oxygen τ_{ox} , water vapor τ_{wv} and clouds τ_{cl} . The hydrometeorological data was collected by the research vessels mainly in the Pacific Ocean and covers a wide range of the variability of the sea surface temperature (SST) t_s , wind speed W , total water vapor content V and total cloud liquid water content Q (Mitnik and Mitnik, 2003) (Table 1).

Table 1. Database Characteristics

Sea surface temperature (°C)	Wind speed (m/s)	Water vapor (kg/m ²)	Cloud liquid water (kg/m ²)
- 1.6 + 31	0 – 30	2.4 – 75.7	0 – 7.07

The calculations were carried out for 50.3- and 52.8-GHz AMSR channels as well as for $\nu = 53.85, 54.8,$ and 55.45 GHz used by SCAMS and AMSU radiometers. Table 2 summarizes the data of numerical experiments.

Table 2. Variations of Total Absorption by Oxygen, Water Vapor, Clouds and the Atmosphere

Frequency (GHz)	Total absorption by:			
	Oxygen	Water Vapor	Clouds	Atmosphere
50.3	0.31-0.35	0.01-0.24	0.0-1.24	0.36-1.25
52.8	1.06-1.10	0.01-0.26	0.0-1.36	1.1-2.7
53.85	2.3-2.4	0.01-0.27	0.0-1.40	2.3-4.1
54.8	5.2-5.4	0.01-0.28	0.0-1.45	5.2-7.0
55.45	8.5-8.8	0.01-0.28	0.0-1.48	8.8-10.3

The T_{BS} variations computed under assumption of the nonscattering atmosphere for the parameter variations shown in Table 1 were equal $\approx 240-275$ K at $\nu = 50.3$ GHz and $\approx 240-267$ K at $\nu = 50.3$ GHz.

From analysis of the microwave radiative transfer equation it follows that the increase of oxygen absorption τ_{ox} produces the redistribution of contributions of the oceanic and atmospheric components to the $T_B(\nu, \theta)$. As τ_{ox} increases, an ocean surface component $\kappa^{V,H}(\nu, \theta) T_o e^{-\tau_{sec\theta}}$ decreases and the outgoing atmosphere component $T_{Batm}^{\uparrow}(\nu, \theta)$ increases.

$$T_{Batm}^{\uparrow}(\nu, \theta) = \int_0^H T(h) K(\nu, h, \theta) dh \quad (2)$$

where $T(h)$ = vertical profile of the atmosphere temperature, h = height above the sea level,

$$K(\nu, h, \theta) = \gamma(\nu, h, \theta) e^{-\int_h^{\infty} \gamma(\nu, h') \sec \theta dh'} \sec \theta$$

= temperature weighting function, and
 γ = atmospheric absorption.

The weighting functions shown in Fig. 1 for the tropical cloudless and cloudy atmospheres viewed at $\theta = 55^\circ$ over the ocean with $t_s = 28^\circ\text{C}$ characterize the degree to which each atmospheric layer contributes to the radiances viewed from space at the indicated frequencies. These weighting functions approach zero at high heights where the atmosphere becomes transparent, or at low heights for those frequencies where the overlying atmosphere is so thick as to be fully opaque.

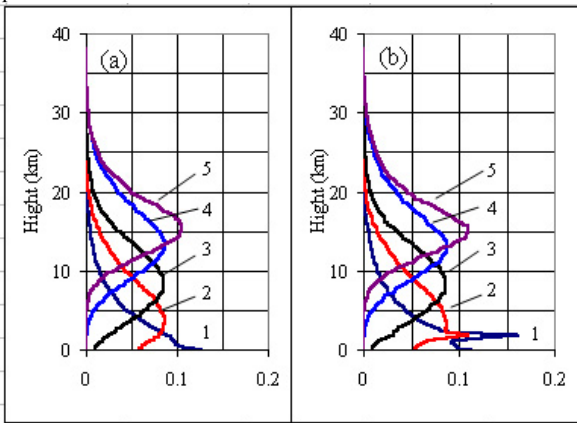


Figure 1. Weighting functions for the tropical atmosphere: at clear sky (a) and at cloudiness with $Q = 0.14 \text{ kg/m}^3$ (b) at frequencies: 1 - 50.3, 2 - 52.8, 3 - 53.8, 4 - 54.8, 5 - 55.4 GHz

Absorption by clouds is high at 50-55 GHz and a cloud layer changes the $K(\nu, h)$ shape (Fig. 1b). Influence of cloudiness on $K(\nu, h)$ and thus on $T_B(\nu)$ depends both on cloud liquid water content and on its height (temperature of cloud droplets).

Although the $T_B(\nu, \theta)$ variations at AMSR oxygen channels are determined by the lower troposphere characteristics they depend also on $T(h)$ and absorption of the middle troposphere especially at $\nu = 52.8$ GHz for which $K(h)$ maximum falls on $h = 3-5$ km and a width of $K(h)$ is about 10 km (Fig. 1). These features in combination with a high resolution permit to detect and to measure the warm anomaly in the TC center.

3. MARINE WEATHER SYSTEMS

ADEOS-II AMSR-E observations are available for a period of 18 January – 23 October 2003 only. Four weather systems were selected for analysis of the T_{BS} features at AMSR-E frequencies: cold air outbreak, mesoscale convective eddy, one extratropical and two tropical cyclones.

3.1 Cold air outbreak

Satellite observations of the Okhotsk Sea during cold air outbreak were carried out on 18 January 2003. Cold Siberian air masses traveling over the warmer sea surface produced an unstable boundary layer of the atmosphere. The cloud streets and mesoscale convective cells (MCCs) of different sizes were clearly revealed on infrared and visible images obtained from NOAA, GMS-9, Terra and Aqua satellites as well as on ADEOS-II AMSR and Aqua AMSR-E microwave images. Fig. 2 shows fields of T_{BS} at 89 GHz with H-polarization and at 50.3 GHz with V-polarization.

Mesoscale convective rolls and cells are the most abundant forms of the organized mesoscale structures and play a very important role in the exchange of momentum and heat between the atmosphere and the ocean surface. They are accompanied by the organized variations of the surface wind. The individual rolls and cells are clearly visible in the $T_B(89H)$ field (Fig. 2a): the wavelength Λ of convective rolls (the distance between neighboring rolls) is 10-20 km to the southeast of ice edge in the Okhotsk Sea and the size of the individual MCCs over the Pacific Ocean is $\approx 20-30$ km.

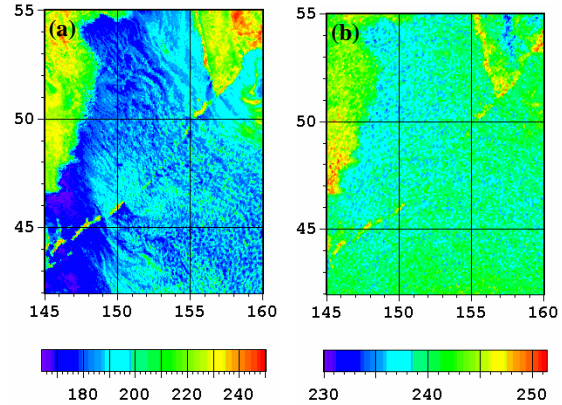


Figure 2. Brightness temperature variations over the Okhotsk Sea and the Pacific Ocean to the east of Kuril Islands caused by mesoscale convective rolls and cells as measured by ADEOS-II AMSR at 89.0 GHz (H-pol) (a) and at 50.3 GHz (V-pol) (b) on 18 January 2003 at 11:17 UTC.

The MCCs and rolls are hardly distinguished in $T_B(50V)$ (Fig. 2b) that can be explained by two factors: the small $T_B(50V)$ increments induced by roll/cell cloudiness and the increased absorption of the atmosphere above the boundary layer. At 52.8 GHz mesoscale convective clouds in the marine boundary layer of the atmosphere were not delineated.

3.2 Convective eddy

Mesoscale convective eddies are usual over the ocean during cold season. Eddies are not always displayed on the weather maps in spite of they are accompanied by strong winds and precipitation. Fig. 3 shows convective eddy near ice edge in a central part of the Okhotsk Sea. It is reliably detected in the fields of the brightness temperatures at all frequencies except 52.8 GHz since eddy's water clouds were very likely located in the lower troposphere.

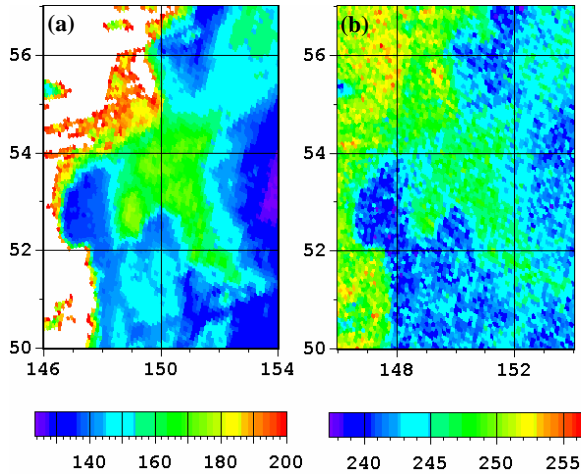


Figure 3. Mesoscale convective eddy near ice edge in the Okhotsk Sea detected by ADEOS-II AMSR at $T_B(36V)$ (a) and $T_B(50V)$ on 2 February 2002 at 00:56 UTC.

3.3 Extratropical cyclone

Quantitative characteristics of southern cyclone in the Japan Sea were estimated with the using of ADEOS-II AMSR, Envisat ASAR, QuikScat SeaWinds and NOAA AVHRR data. $T_B(19H)$ (a) and $T_B(50V)$ (b) images shown in Fig. 4 reflect spatial distribution of the atmospheric and ocean surface parameters influencing on spectrum of the brightness temperature: total cloud liquid water content Q , total water vapor content V and wind speed W . These parameters were retrieved with algorithms given in (Mitnik and Mitnik, 2003). The central area of the cyclone the size of ≈ 100 km around $37^\circ N$, $132^\circ E$ is characterized by weak winds, the absence of water clouds and the decreased V -values (≈ 20 kg/m³). The strongest winds (≈ 15 -20 m/s) are observed in the area of the secondary cold front the width of ≈ 200 km located to the north and northeast of the cyclone center. Q -values are increased with the $T_B(18V)$ increase: $Q = 0.1$ -0.5 kg/m² at $T_B(18V) \approx 130$ -155 K, $Q = 0.8$ -1.2 kg/m² at $T_B(18V) \approx 160$ -180 K. Probability of precipitation is high at $Q > 0.5$ -07 kg/m². The intensive rains are observed at $T_B(18V) > 190$ K.

$T_B(50V)$ ranges in value from ≈ 240 to ≈ 268 K and reveals a spatial structure of the cyclone at less details as compared to T_B at $\nu = 18$ -37 GHz. Variability of $T_B(53V)$ is small (≈ 8 K only) and the features of cyclone structure are not seen.

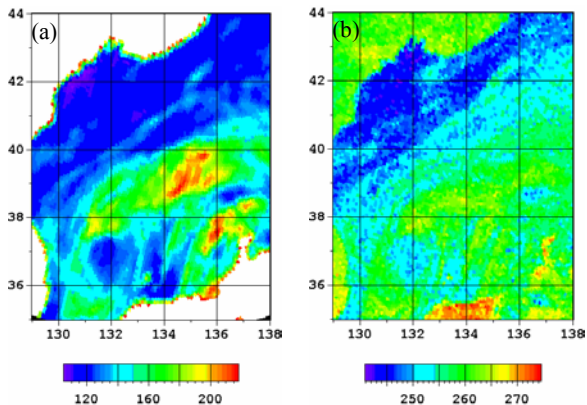


Figure 4. Cyclone over the southern Japan Sea: $T_B(19H)$ (a) and $T_B(50V)$ (b) taken on 8 April 2003 at 02:00 UTC.

3.4 Tropical cyclone

The warm anomaly in the eye area, the cold eye wall, spiral rain bands and other features of the Pacific and Atlantic tropical cyclones were detected by ADEOS-II oxygen channels. Figs. 5a,b shows hurricane Isabel in the Atlantic Ocean as it was seen by the AMSR oxygen channels on 11 September 2003 at 03:20 UTC.

The sections crossing hurricane's center from the west to the east show that the eye's T_B values exceed the background level on ≈ 15 K at $\nu = 50.3$ GHz and on ≈ 7 K at $\nu = 52.8$ GHz. The size of the warm core is ≈ 30 km (at 52.8 GHz). Narrow negative peaks with $T_B < 250$ K correspond to eye wall crossing (Figs. 5c,b). Diameter of cold eye wall is ≈ 65 -70 km. The area surrounding the eye is also characterized by low T_B s due to scattering of microwave radiation by large rain droplets and hail that is typical for central continuous dense cloud massif. Its diameter is ≈ 200 km. The T_B s values grow as the distance from the hurricane's center increases. The spiral rain bands are also detected by both oxygen channels. Their brightness contrasts against the background may be both positive and negative and depend on vertical profiles of precipitation, cloud liquid water content and air temperature.

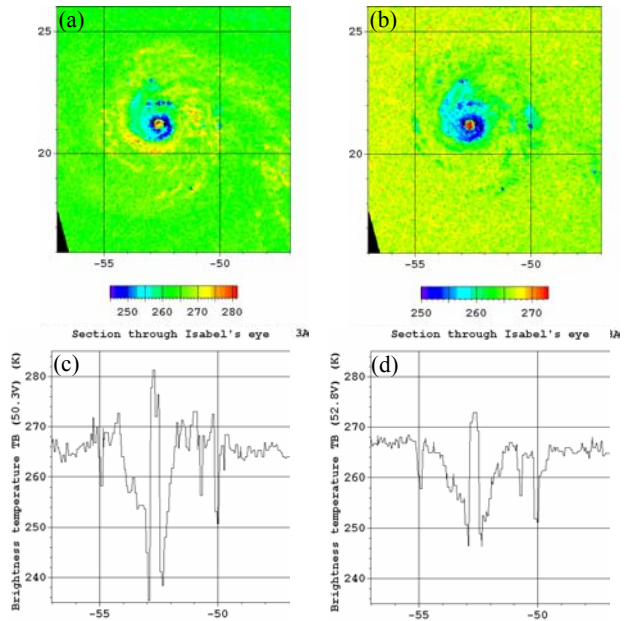


Figure 5. ADEOS-II AMSR sensing of Hurricane Isabel on 11 September 2003 at 03:20 UTC. T_B images (a) and (b) and sections through the hurricane's eye (c) and (d) at 50.3 GHz (a) and (c) and at 52.8 GHz (b) and (d).

4. CONCLUSIONS

The main parameters of satellite microwave radiometer which determine the possibility of detection and quantitative estimate of the

structural features of the various marine weather systems are the frequency, polarization and IFOV of radiometer's channels.

The results of numerical experiments with a model of microwave radiative transfer with the using of global hydrometeorological database have shown that at $\nu = 50.3$ GHz total absorption by oxygen is between 0.3-1.1 that considerably more than at other AMSR channels, total water vapor absorption is ≈ 1.7 times greater than at $\nu = 36.5$ GHz and water cloud absorption is ≈ 1.6 -2.0 times greater than at $\nu = 36.5$ GHz.

Maxima of the weighting functions $K(h,\nu)$ showing contribution of different atmospheric layers to the $T_B(\nu)$ are located at the sea level ($h = 0$ km) at $\nu = 50.3$ GHz and at $h \approx 2$ -3 km at $\nu = 52.8$ GHz. Their width $\Delta h \approx 5$ km ($\nu = 50.3$ GHz) and 10 km ($\nu = 52.8$ GHz).

The 50.3 and 52.8-GHz channels provided new and interesting data on the marine weather systems and temperature structure of tropical cyclones. In particular a warm anomaly of the eye in the Atlantic hurricanes and Pacific typhoons of the 2003 season as well as the detailed structure of the eye wall was reliably measured due to a high spatial resolution of ADEOS-II AMSR oxygen channels. These experimental data and the results of modeling at other frequencies within 5-mm oxygen absorption band clearly demonstrate the advantages of high-resolution satellite measurements for study the TCs and other weather systems and call for further investigation.

5. ACKNOWLEDGEMENTS

This study has been carried out within the cooperation between the Japan Aerospace Exploitation Agency (JAXA) and the V. I. Il'ichev Pacific Oceanological Institute, Far Eastern Branch of the Russian Academy of Sciences in the ADEOS-II Research activity (project A2ARF006). This work is partially sponsored by a grant for a project: "Investigation of ocean-atmosphere system with passive and active microwave sensing from new generation of satellites" from the FEB RAS.

6. REFERENCES

S.Q. Kidder, W.M. Gray, and T.H. Vonder Haar, "Estimating tropical cyclone central pressure and outer winds from satellite microwave data", *Monthly Weather Review*, vol. 106, p.p. 1458-1464, 1978.

S.Q. Kidder, M.D. Goldberg, R.M. Zehr, M. DeMaria, J.F.W. Purdom, C.S. Velden, N.C. Grody, and S.J. Kusselson, "Satellite analysis of tropical cyclones using the Advanced Microwave Sounding Unit (AMSU)", *Bull. Amer. Meteor. Soc.*, vol. 81, p.p. 1241-1259, 2000.

L.M. Mitnik, and M.L. Mitnik, "Retrieval of atmospheric and ocean surface parameters from ADEOS-II Advanced Microwave Scanning Radiometer (AMSR) data: Comparison of errors of global and regional algorithms", *Radio Sciences*, vol. 38, No. 4, 8065, doi: 10.1029/2002RS002659, 2003.

P. W. Rosenkranz, D.H. Staelin and N.C. Grody, "Typhoon June (1975) viewed by a Scanning Microwave Spectrometer", *J. Geophys. Res.*, vol. 3, No. C4, p.p. 1857-1868, 1978.

D.H. Staelin, and F.W. Chen, "Precipitation observations near 54 and 183 GHz using the NOAA-15 Satellite", *IEEE Trans. Geosci. Rem. Sens.*, vol.38, No.5, p.p.2322-2332, 2000.

C.S. Velden, and W.L. Smith, "Monitoring tropical cyclone evolution with NOAA satellite microwave observations", *J. Clim. Appl. Meteor.*, vol. 22, p.p. 714-724, 1983.

J.A. Knaff, R.M.Zehr, M.D.Goldberg, and S.Q.Kidder, "An example of temperature structure differences in two cyclone systems derived from the Advanced Microwave Sounding Unit", *Weather and Forecasting*, vol. 15, p.p. 476-483, 2000.

C.S. Velden, "Observational analyses of North Atlantic tropical cyclones from NOAA polar-orbiting satellite microwave data", *J. Appl. Meteor.*, vol. 28, p.p. 59-70, 1989.

C.S. Velden, B.M. Goodman, and R.T. Merrill, "Northwest Pacific tropical cyclone intensity estimation from NOAA polar-orbiting satellite microwave data", *Monthly Weather Review*, vol. 119, p.p. 159-168, 1991.